Proceedings of Anticancer Research

Research Article

^{99m}Tc Radiolabeled Archaeosomes as a Potential Melanoma Imaging Agent

Mirel Cabrera[1]*, Marcos Tassano[1], Marcelo Fernández[1], Juan Pablo Gambini[2], Pablo Cabral[1]*

[1]Area de Radiofarmacia, Centro de Investigaciones Nucleares, Facultad de Ciencias, Universidad de la República. Mataojo 2055, 11400 Montevideo, Uruguay, [2]Centro de Medicina Nuclear, Hospital de Clínicas "Dr. Manuel Quintela", Facultad de Medicina, Universidad de la República. Av. Italia s/n, 11600, Montevideo, Uruguay

Abstract: Melanoma incidence is growing worldwide. Although recent advances in imaging, there is not still available a specific melanoma agent that can be used for melanoma staging. Archaeosomes may be defined as liposomes composed of one or more polar lipids extracted from the Archaea domain (*Archaebacterium*). As liposomes have been used as vehicles for drugs and isotopes, the aim of this work is to evaluate radiolabelled 99mTc-archaeosomes as a potential melanoma imaging agent. and evaluate its potential role as a melanoma imaging agent. Archaeosomes were prepared by handshaken method and were radiolabeled with ^{99m}Tc; radiolabelling efficiency and purity were evaluated through different chromatographic systems. *In vitro* stability of ^{99m}Tc-diethylene-triamine-pentaacetate (DTPA)-archaeosomes was performed through L-cysteine challenge. Archaeosome size distribution was determined by laser light scattering, having nanometer size between 90 and 120 nm. Radiolabelling efficiency was >90%; ^{99m}Tc-DTPA-archaeosomes presented a radiochemical purity superior to 80% evaluated 24 h post-radiolabelling. For the highest concentration of L-cysteine (30 mM) and 1 h incubation, radiochemical purity was 92.90%, 6.41% was bound to cysteine, and 0.69% remained as $^{99m}TcO_4^-$. Biodistribution and scintigraphic imaging studies in healthy C57 black mice showed high liver, spleen uptake, and renal elimination. Melanoma bearing mice had similar biodistribution as healthy mice but increased melanoma uptake, with T/M ratio of 46 ± 3.7. Our results show the feasibility of ^{99m}Tc radiolabelling archaeosomes and their potential role as a melanoma imaging agent.

Key words: *^{99m}Tc-archaeosomes, melanoma, tumor imaging.*

Publication date: May 2018

Publication online: 31st May 2018

Corresponding Authors: Mirel Cabrera and Pablo Cabral, pcabral@cin.edu.uy

0 Introduction

Archaeosomes may be defined as liposomes composed of one or more polar lipids extracted from Archaea domain (*Archaebacterium*). Although Archaea and Bacteria are both prokaryotes, Archaea is more closely related to Eucarya domain than bacteria[1]. Archaea polar lipids can be composed by a core of archaeol or caldarqueol, or a mixture of both[2], structures of archaeobacterial membrane lipids[3]. Polar heads lipids (phospho glycol, amine, and hydroxyl) of Archaea are similar to those found in phosphatidylcholine from Eukaryotes and Bacteria; however, esther lipids are rarely seen in Archaea. Archaeol membrane lipids are monopolar and caldarchaeol lipids are bipolar. Archea extracts have a net negative charge, due to the predominance of negatively polar head groups in the lipids[2]. In the same way as phospholipids, archaeolipids, in contact with water form flat bilayers that with the addition of energy, are sealed and form vesicles[4].

Liposomes are more susceptible to hydrolysis by the presence of ester bonds, oxidation due to the presence of unsaturations, and content loss. Otherwise, archeosomes have greater structural strength in hostile environments[5]. Therefore, archeosomes may play an interesting role in chemotherapy as a potential drug carrier[6-9]. It has also been reported that archaeosomes

have an important adjuvant activity *in vivo*[10]. This adjuvant activity correlates to macrophages and dendritic cells recruitment and activation. If archeosomes can be used to deliver drugs to tumors, they could also be radiolabeled to be used as an imaging agent. The aim of this work is to evaluate radiolabelled ^{99m}Tc-archaeosomes as a potential melanoma imaging agent.

2 Materials and methods

2.1 Archaeosomes synthesis

Archaeosomes were prepared by handshaken method[11,12]. *Halorubrum tebenquichense* Archae lipids were extracted from frozen and thawed biomass, with Cl_3CH:CH_3OH:H_2O (1:2:0.9; v: v), and the total polar lipid fraction was collected by precipitation from cold acetone (kindly donated by PhD. Eder Romero Laboratory UNQ, Argentina).

Typically 11 mg of extracted lipids from Archaea and 2 mg estearilamide-diethylene-triamine-pentaacetate (DTPA) (in-house synthesis) were added in chloroform-methanol (2: 1 v/v) medium to a round bottom flask. Lipids were rota-evaporated to dryness in 60°C water bath at 120 rpm. The obtained film was hydrated with 5 ml of bidistilled water. Then, multilamellar large vesicles obtained were extruded through a series (11, 0.4 μm, and 11, 0.2 μm) of polycarbonate filters to form unilamellar archaesomes. Particle size distribution was determined by laser light scattering Nano Zetasizer ZS (Malvern) located at Facultad de Química, UdelaR.

2.2 Radiolabelling and physicochemical controls

Pre-formed archaeosomes were radiolabelled with ^{99m}Tc. To do so, 2.0 mL suspension of previously extruded archaeosomes was added 0.3 mL of SnF_2 (0.69 mg/ml) and $^{99m}TcO_4^-$ 185–259 MBq (5–7 mCi). The mixture was incubated for 20 min at room temperature. Radiochemical purity was determined through the following chromatographic systems: ITLC-SG/NaCl 0.9% (Rf:$^{99m}TcO_4^-$ = 0.9–1.0; other species Rf = 0. 0); ITLC-SG/Pyr: HAc: H_2O (Rf$^{99m}TcO_2.xH_2O$ Rf = 0. 0, other species Rf = 9 0–1.0); and molecular exclusion chromatography PD-10 Sephadex G25, solvent NaCl 0.9%, taken fractions of 0.5 mL.

2.3 *In vitro* stability

^{99m}Tc-archaeosomes (0.4 mL) prepared as previously described were challenged against 0.4 mL of different solutions of L-cysteine (Sigma)[13-15]. The final concentrations of L-cysteine obtained were 0.1, 10, and 30 mM. Different mixtures were incubated for 3 h at 37°C. Controls were carried out in the following chromatographic systems: ITLC-SG/NaCl 0.9% (Rf:$^{99m}TcO_4^-$ = 0.9-1.0, Rf^{99m}Tc-Cys = 0.9–1.0, other species Rf = 0.0); ITLC-SG/Pyr: HAc: H_2O (Rf$^{99m}TcO_2.xH_2O$ Rf = 0.0, other species Rf = 0.9–1.0); and Whatman 1/2-Butanone (Rf:$^{99m}TcO_4^-$ = 0.9–1.0, Rf = 0.0 other species). The activity of each fraction of the strip was measured in a solid scintillation counter: With a glass of NaI (Tl) 3 “x 3” coupled to a detector with single-channel Analyzer (ORTEC).

2.4 Cell culture and animal model

B16-F1 murine melanoma cell line obtained from the American Type Culture Collection was maintained in Dulbecco’s modified Eagle’s medium (PAA Laboratories GmbH, Pasching, Austria) supplemented with 10% fetal bovine serum (PAA Laboratories GmbH) and 2 mM glutamine (AppliChem GmbH, Darmstadt, Germany). 6-week-old C57BL/6 mice (URBE, Uruguay) were used in all experiments. Melanomas were induced in mice by subcutaneous injection of 2.5×10^5 B16-F1 melanoma cells in 0.1 ml of phosphate-buffered saline in the right flank. After 2 weeks of inoculation, tumors were palpable (1 cm^3) and mice were ready for biodistribution and scintigraphic studies. All mentioned protocols were approved by our Animal Experimentation National Committee for (CHEA, Uruguay).

2.5 Biodistribution studies

Biodistribution studies were carried out after intravenous injection of ^{99m}Tc- archaeosomes 6.5 ± 1.2 MBq (176 ± 33 μCi) in physiological serum as vehicle to melanoma bearing mice, as well as to C57BL/6 normal mice. Biodistribution was performed at 4 h and 24 h, and 8 animals were used by time point (4 normal mice and 4 melanoma bearing mice). Animals were sacrificed by cervical dislocation; tissues and organs of interest were harvested and washed with distilled water to remove blood excess and weighted. Activity was measured using a solid scintillation counter (ORTEC), and the activity found in each organ was presented as a percentage of the total dose injected per gram (%DI/g) of tissue or organ. To calculate the gross correlation between the distribution of normal mice and melanoma bearing mice, it was compared the acquisition of

^{99m}Tc-arqueosomas expressed as a percentage of the injected dose % ID.

2.6 Images

Scintigraphic images were carried out in normal and melanoma bearing C57BL/6 mice (n = 4). Images were acquired with a gamma camera (model Sophy DSX, Sopha Medical, Buc, France, connected in series with a computational system, Mirage Segami, Columbia, MD). The equipment consisted of a large field of view rectangular gamma camera (Sophy DSX, Sopha Medical) fitted with a low-energy, high-resolution collimator. Planar images of mice were acquired on a 256 × 256 matrix, using a 15% window centered on an energy peak of 140 keV. Mice were injected with 22.2 MBq (0.6 mCi) of ^{99m}Tc-archaeosomes through tail vein and anesthetized by intraperitoneal injection of ketamine-Xilazina (100–10 mg/kg). Mice were imaged 4 h post-administration of the radiolabelled compound. Region of interest (ROI) was placed over tumor region and compared against contralateral flank (tumor/healthy tissue ratio).

3 Results

3.1 Characterization of the archaeosomes

Archaeosome size distribution was determined by laser light scattering Nano Zetasizer ZS, having nanometer size between 90 and 120 nm [Figure 1].

Radiolabelling efficiency and purity were evaluated through the mentioned chromatographic systems, having a radiolabelling efficiency >90%.^{99m}Tc-DTPA-archaeosomes presented a radiochemical purity superior to 80% evaluated 24 h post-radiolabelling. Furthermore, archaeosomes in the molecular exclusion chromatography (column PD-10 G-25) were obtained at 3.0–3.5 mL of elution while $^{99m}TcO_4^-$ was eluted at 6.0–6.5 mL.

3.2 *In vitro* stability

In vitro stability of ^{99m}Tc-DTPA-archaeosomes was performed through L-cysteine challenge. At 0.1 mM cysteine concentration and 1 h incubation, 96% ± 2.1 ^{99m}Tc remained attached to archaeosomes, 0.82 ± 0.09% was bound to cysteine, and 3.15 ± 0.16% remained as $^{99m}TcO_4^-$. At 3 h of incubation, 96.3 ± 1.8% of ^{99m}Tc remained bound to archaeosomes, while 0.11 ± 0.01% and 2.55± 0.13% were attached to cysteine and $^{99m}TcO_4^-$, respectively. At 10 mM cysteine concentration and 1 h incubation, radiochemical purity was 91 ± 2.0%, while 3.2 ± 0.1% and 6.4 ± 0.08% of ^{99m}Tc were attached to cysteine and $^{99m}TcO_4^-$, respectively, at 3 h of incubation, 70.9 ± 1.6% ^{99m}Tc remained attached to archaeosomes, 28 ± 1.3% was bound to cysteine, and 1.1 ± 0.05% remained as $^{99m}TcO_4^-$. For the highest concentration of cysteine (30 mM) and 1 h incubation, radiochemical purity was 92.90 ± 7.01%, 6.41 ± 0.19% was bound to cysteine, and 0.69 ± 0.12% remained as $^{99m}TcO_4^-$. At 3 h of incubation, 64.9 ± 3.17% of ^{99m}Tc remained bound to archaeosomes, while 32 ± 0.38% and 3.1 ± 0.13% were attached to cysteine and $^{99m}TcO_4^-$, respectively [Figure 2].

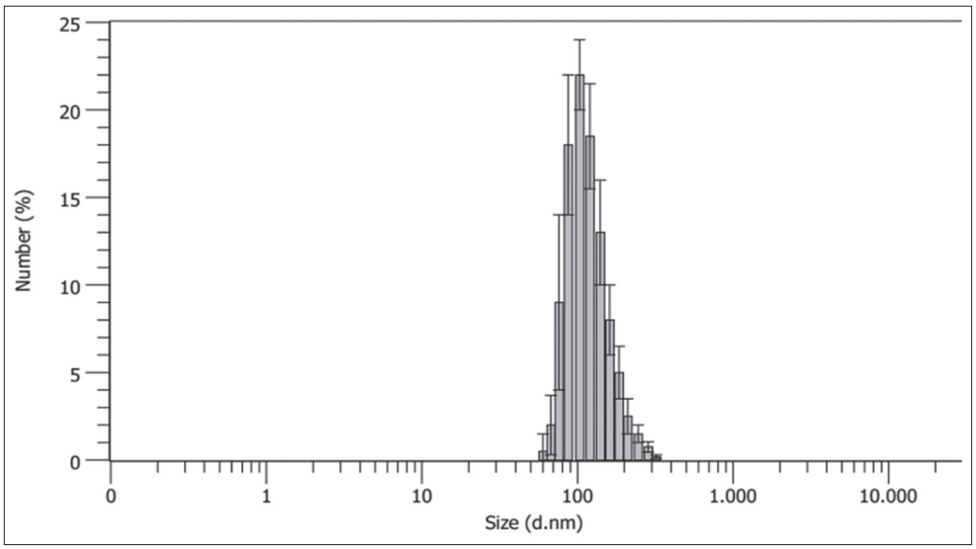

Figure 1. Hydrodynamic diameter of archaeosomes measured by dynamic light scattering expressed in number mode (Zetasizer Nano ZS, Malvern). The graph shows the results of measuring 10 times the same sampled of archaeosomes.

3.3 Biodistribution studies

Biodistribution results of ^{99m}Tc-DTPA-archaeosomes in normal C57BL/6 mice at 4 h and 24 h are shown in Figure 3. These studies show that ^{99m}Tc-DTPA-archaeosomes have an important hepatic uptake (17.72% ± 5.4 and 25.43% ± 4.0) at 4 and 24 h, respectively. Furthermore, it was evidenced spleen uptake (10.84% ± 0.7 and 14.71% ± 2.3) at 4 and 24 h, respectively. Kidney uptake was 4.45% ± 1.25 and 3.02% ± 0.29 at 4 and 24 h, respectively. These results are consistent with a high blood clearance at 4 h (0.93% ± 0.37), showing low activity blood levels at 24 h (0.92% ± 0.37%).

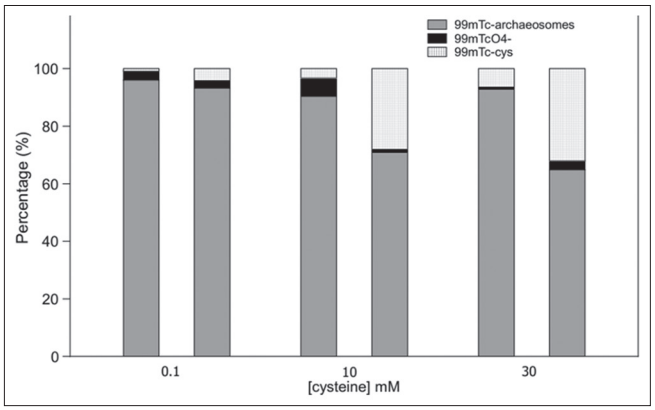

Figure 2. Stability study of ^{99m}Tc-diethylene-triamine-pentaacetate-archaeosomes evaluated through cysteine challenge at 1 h (a) and 3 h (b) at 37°C, respectively.

Melanoma bearing mice presented a similar biodistribution pattern than the one observed in normal C57BL/6 mice. It was also observed high liver (19.0 ± 6.5 and 19.4% ± 1.89) and spleen uptake (13.36 ± 0.24 and 3.62 ± 1.56) at 4 and 24 h, respectively [Figure 4]. Kidney uptake was 2.54% ± 1.62 at 4 h and 3.0 ± 1.0% at 24 h. At 24 h, tumor uptake was 0.83 ± 0.27, with a tumor/muscle ratio of 5 at 4 h, increasing to a ratio of 34 at 24 h.

3.4 Images

Scintigraphic studies of ^{99m}Tc-DTPA-archaeosomes in C57BL/6 normal and melanoma-bearing mice at 4 hshow important abdominal uptake that correlates with liver, spleen, and kidney uptake. Furthermore, bladder activity was observed in both the studies. In melanoma-bearing mice, there was an important tumor uptake. ROI (tumor/healthy tissue) ratio was 46.6 ± 3.7 [Figure 5].

4 Discussion

Cancer of the skin is by far the most common of all cancers. It is estimated that the annual increase in the incidence rate of melanoma has been approximately 3–7% per year worldwide for Caucasians[16]. Concerning melanoma mortality by 2012, Europe's rate of 1.5/100 000 (person-years) is the third highest in the World,

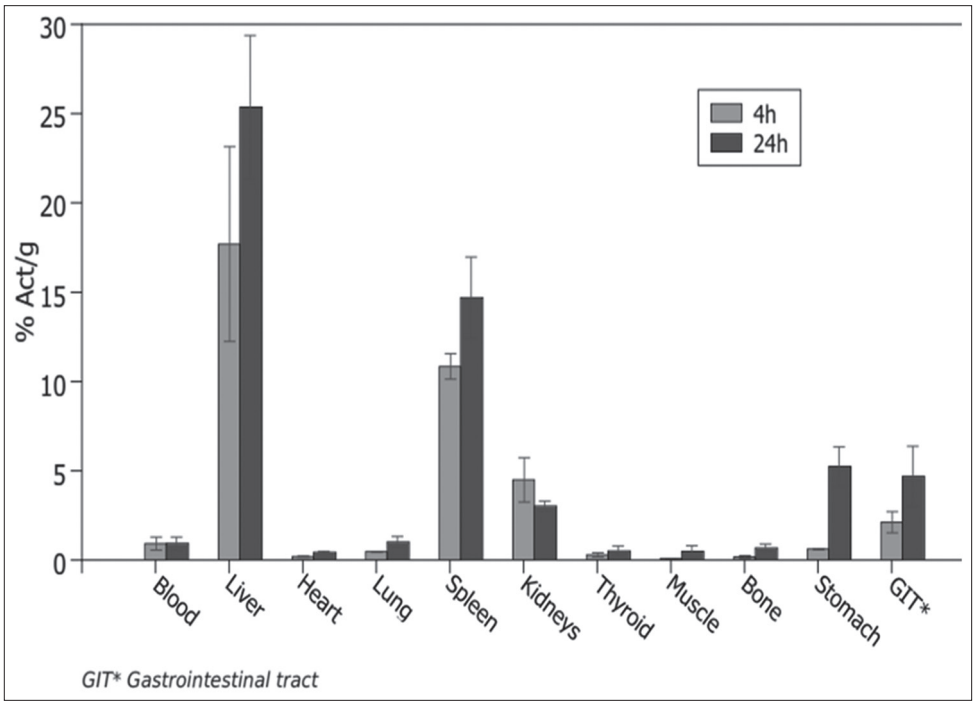

Figure 3. Biodistribution study in normal C57BL/6 mice (n = 4), at 4 h and 24 h post-injection of ^{99m}Tc-diethylene-triamine-pentaacetate-archaesosomes. Results are presented as % Act/g mean and ±1 standard deviation error bar.

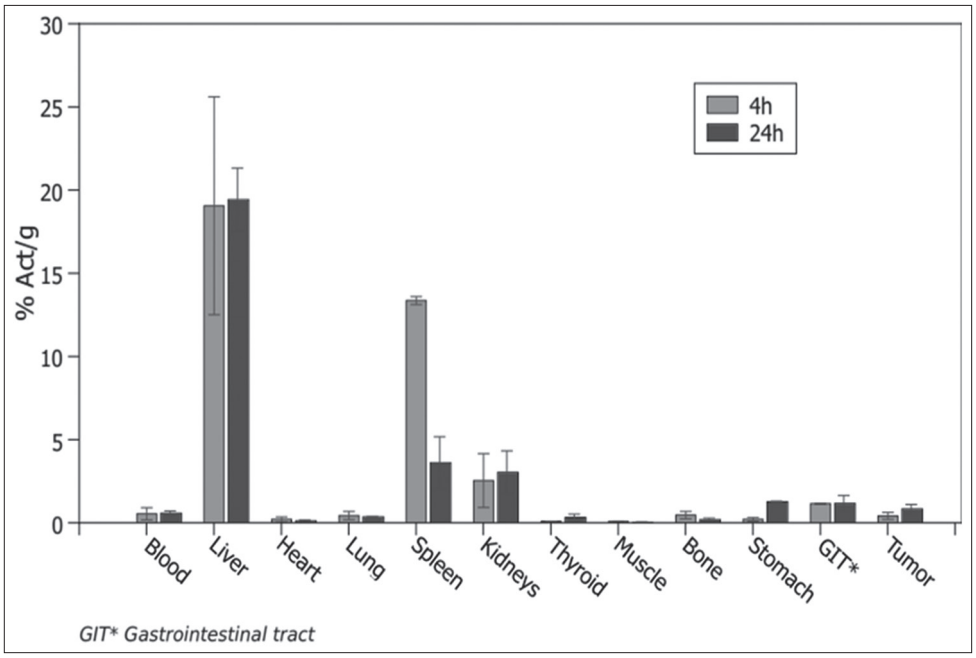

Figure 4. Biodistribution study in C57BL/6 melanoma-bearing mice (n = 4), at 4 h and 24 h post-injection of ^{99m}Tc-diethylene-triamine-pentaacetate-archaesosomes. Results are presented as % Act/g mean and +/−1 standard deviation error bar

after Australia/New Zealand (3.5/100 000) and North America (1.7/100 000) [17].

Studies have confirmed that extensive radiologic studies such as computed tomography (CT), magnetic resonance imaging (MRI), positron emission tomography (PET), PET-CT, and bone scans have an extremely low yield in asymptomatic patients with primary cutaneous melanoma and are generally not indicated[18,19]. These results highlight the need of novel imaging modalities or tracers able to stage melanoma patients. In this way, we have developed ^{99m}Tc radiolabeled archaeosomes aiming to be used as a melanoma imaging agent. Our results demonstrate that archaeosomes can be synthesized using a similar approach as the one described to syntethize liposomes[20].

We also observed that ether polar lipids of archaeobacteria can be used in either a fluid or a liquid-crystalline state[21]. Therefore, it is possible to work in the film hydration phase at room temperature, thus simplifying its synthesis. Another advantage of these lipids is that they do not oxidate in the presence of air since phytane chains are saturated. This allows us to store them at room temperature and in the presence of oxygen. In addition, these lipids are characterized by high thermal stability[22], so they can be sterilized by autoclave which is an advantage for their *in vivo* applications.

Radiolabelling DTPA-archaeosomes were achieved following the simple procedure at room temperature,

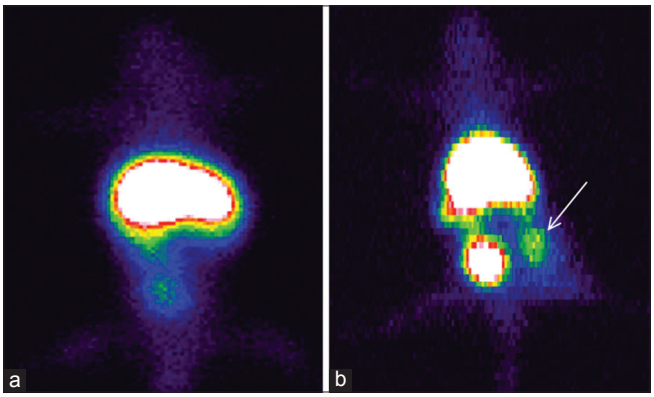

Figure 5. Scintigraphic images at 4 h post-injection of ^{99m}Tc-diethylene-triamine-pentaacetate-archaeosomesin C57BL/6 normal (a) and melanoma-bearing mice (b). Arrow in B indicates tumor uptake

resulting in 90% of PRQ, maintained superior to 80% at 24 h post-labelling. ^{99m}Tc-DTPA-archaeosomes were challenged against increased concentration of cysteine, being stable at all concentrations studied at 1 h. Even with a concentration of 0.1 mM at 3 h, radiochemical purity was superior to 90%. At higher cysteine concentrations than the ones found in plasma (10 and 30 mM), radiolabeled archaeosomes were not so stable [Figure 2][23].

In terms of *in vivo* stability, this system proved to have a high blood clearance due to mononuclear phagocyte system capture as biodistribution and scintigraphic images show. There is high liver (25.36 ± 4.0 and 19.41 ± 1.9) and spleen (14.69 ± 2.3 and 3.61 ± 1.5)

uptake in normal and melanoma-bearing mice, and also, there are elements of biliary excretion that explains the intestinal activity. Furthemore, we found lesser degree elements of urinary elimination (kidney and bladder uptake). Liver and spleen uptake is not due to blood destabilization caused by high-density lipoproteins (HDL), as seen with liposomes. HDL is responsible for the removal from liposomes of the phospholipids present in the outer side of the bilayer formed by ester like lipids[24]. Furthermore, archaesomes present ether bonds, while liposomes have ester bonds. It should be mentioned that the radioactive complex itself is stable *in vivo*, without evidencing a change in ^{99m}Tc-DTPA-archaesomes biodistribution profile [Figures 3 and 4][25]. Biodistribution studies of melanoma-bearing mice at 4 and 24 h showed tumor uptake, having a tumor/muscle (T/NT) ratio of 5 at 4 h and 34 at 24 h with high blood clearance. These results are comparable to the ones reported for radiolabeled antibodies for tumor detection[26].

Similar results were found in scintigraphic images, were tumor/muscle (T/NT) ratio was approximately 46 at 4 h. We also found abdominal uptake due to mainly liver, spleen, and gastrointestinal activity without considerable muscle uptake. Arcaheosomes melanome accumulation maybe due to enhanced permeability and retention effect (EPR). This effect is highly dependent on size, being more effective between 100 and 200 nm[27]. Our synthetized ^{99m}Tc radiolabeled archaeosomes range from 90 to 120 nm making EPR possible.

^{99m}Tc-DTPA-archaeosomes showed higher tumor-specific accumulation, compared to similar ^{99m}Tc-DTPA-liposomes, where T/M ratio was approximately 4 at 4 h while in radiolabeled archaeosomes was 46[20]. This striking difference may be due to EPR effect and also by macrophages present in tumor microenvironment that are involved in their elimination. Macrophages do not recognize liposomes[28]. If so, ^{99m}Tc radiolabeled archaeosomes could be used for sentinel node procedures. This hypothesis will be studied in depth in future research.

Taking into account ^{99m}Tc-DTPA-archaeosome biodistribution and scintigraphic images, maybe it would be of interest to use it as a head and neck melanoma agent due to the fact of the low uptake in these structures and the high melanoma uptake. We must consider the high incidence of this kind of tumors, 10–20% of all cutaneous melanomas arise in the head and neck region, the incidence in this area has similarly increased, from 2 per 100,000 in 1996 to 2.7 per 100,000 in 2001[29].

5 Conclusion

Our results describe, for the first time, the feasibility of ^{99m}Tc radiolabeling of archaeosomes. It was performed in an easy and simple way, and our results indicate that it can be used as a potential melanoma imaging agent, highlighting its potential role in head and neck melanomas. Furthermore, these same concepts could be applied to other solid tumors and for sentinel node procedures.

6 Conflict Of Interest

The authors declares that there is no conflict of interest regarding the publication
of this paper.

7 Acknowledgements

- Agencia Nacional de Investigación e Innovación (ANII) Uruguay.
- Department of Science and Technology, National University of Quilmes.Quilmes, Buenos Aires, Argentina.

References

[1] Krieg NR. Procaryotic Domains: In Bergey's Manual of Systematic Bacteriology. New York: Springer-Verlag; 2001. p. 21-5.

[2] Sprott GD. Structures of archaeobacterial membrane lipids. J Bioenerg Biomembr 1992;24:555-66.

[3] Kates M. Archaebacterial lipids: Structure, biosynthesis and function. Biochem Soc Symp 1992;58:51-72.

[4] Krishnan L, Sad S, Patel GB, Sprott GD. Archaeosomes induce long-term CD8+ cytotoxic T cell response to entrapped soluble protein by the exogenous cytosolic pathway, in the absence of CD4+ T cell help. J Immunol 2000;165:5177-85.

[5] Li Z, Chen J, Sun W, Xu Y. Investigation of archaeosomes as carriers for oral delivery of peptides. Biochem Biophys Res Commun 2010;394:412-7.

[6] Krishnan L, Dicaire CJ, Patel GB, Sprott GD. Archaeosome vaccine adjuvants induce strong humoral, cell-mediated, and memory responses: Comparison to conventional liposomes and alum. Infect Immun 2000;68:54-63.

[7] Kaur G, Garg T, Rath G, Goyal AK. Archaeosomes: An excellent carrier for drug and cell delivery. Drug Deliv 2016;23:2497-512.

[8] Benvegnu T, Lemiègre L, Cammas-Marion S. New generation of liposomes called archaeosomes based on natural or

synthetic archaeal lipids as innovative formulations for drug delivery. Recent Pat Drug Deliv Formul 2009;3:206-20.

[9] Markelc B, Batista NT, Ota A, Cemazar M, Poklar N, Miklavcic D, *et al*. Archaeosomes Prepared from *Aeropyrum Pernix* K1 Lipids as an *In Vivo* Targeted Delivery System for Subsequent Nanosecond Electroporation. In: 6th European Conference of the International Federation for Medical and Biological Engineering. Springer, IFMBE Proceedings. p45.

[10] Krishnan L, Sad S, Patel GB, Sprott GD. The potent adjuvant activity of archaeosomes correlates to the recruitment and activation of macrophages and dendritic cells *in vivo*. J Immunol 2001;166:1885-93.

[11] Akbarzadeh A, Rezaei-Sadabady R, Davaran S, Joo SW, Zarghami N, Hanifehpour Y, *et al.* Liposome: Classification, preparation, and applications. Nanoscale Res Lett 2013;8:102.

[12] Shaheen SM, Ahmed FR, Hossen N, Ahmed M, Amran S. Liposome as a carrier for advanced drug delivery. Pak J Biol Sci 2006;9:1181-91.

[13] Zhu X, Li J, Hong Y, Kimura RH, Ma X, Liu H, *et al*. 99mTc-labeled cystine knot peptide targeting integrin αvβ6 for tumor SPECT imaging. Mol Pharm 2014;11:1208-17.

[14] Stalteri MA, Bansal S, Hider R, Mather SJ. Comparison of the stability of technetium-labeled peptides to challenge with cysteine. Bioconjug Chem 1999;10:130-6.

[15] Hnatowich DJ, Virzi F, Fogarasi M, Rusckowski M, Winnard P Jr. Can a cysteine challenge assay predict the *in vivo* behavior of 99mTc-labeled antibodies? Nucl Med Biol 1994;21:1035-44.

[16] Parkin DM, Bray F, Ferlay J, Pisani P. Estimating the world cancer burden: Globocan 2000. Int J Cancer 2001;94:153-6.

[17] Forsea AM, Del Marmol V, de Vries E, Bailey EE, Geller AC. Melanoma incidence and mortality in Europe: New estimates, persistent disparities. Br J Dermatol 2012;167:1124-30.

[18] Weiss M, Loprinzi CL, Creagan ET, Dalton RJ, Novotny P, O'Fallon JR, *et al.* Utility of follow-up tests for detecting recurrent disease in patients with malignant melanomas. JAMA 1995;274:1703-5.

[19] Hafner J, Schmid MH, Kempf W, Burg G, Künzi W, Meuli-Simmen C, *et al.* Baseline staging in cutaneous malignant melanoma. Br J Dermatol 2004;150:677-86.

[20] Cabrera M, Medrano A, Lecot N, Moreno M, Chabalgoity JA, *et al*. A Novel Method to Radiolabel Stealth Liposome through 1,2- dimyristoyl-sn-glycero-3-phosphoethanolamine-N-DTPA with 99mTc and Biological Evaluation. Journal of Analytical Oncology 2013;2:1-9.

[21] Koga Y. Thermal adaptation of the archaeal and bacterial lipid membranes. Archaea 2012;2012:789652.

[22] Patel GB, Chen W. Archaeosomes as drug and vaccine nano delivery systems. In: Nanocarrier Technologies: Frontiers of Nanotherapy. Netherlands: Springer; 2006. p. 17-40.

[23] Brigham MP, Stein WH, Moore S. The concentrations of cysteine and cystine in human blood plasma. J Clin Invest 1960;39:1633-8.

[24] Wolfbauer G, Albers JJ, Oram JF. Phospholipid transfer protein enhances removal of cellular cholesterol and phospholipids by high-density lipoprotein apolipoproteins. Biochim Biophys Acta 1999;1439:65-76.

[25] Irwin RS, Doherty PW, Bartter T, Gionet MM, Collins JA. Evaluation of technetium pertechnetate as a radionuclide marker of pulmonary aspiration of gastric contents in rabbits. Chest 1988;93:1270-5.

[26] Paudyal P, Paudyal B, Hanaoka H, Oriuchi N, Iida Y, Yoshioka H, *et al.* Imaging and biodistribution of her2/neu expression in non-small cell lung cancer xenografts with cu-labeled trastuzumab PET. Cancer Sci 2010;101:1045-50.

[27] Kibria G, Hatakeyama H, Ohga N, Hida K, Harashima H. The effect of liposomal size on the targeted delivery of doxorubicin to integrin αvβ3-expressing tumor endothelial cells. Biomaterials 2013;34:5617-27.

[28] Kelly C, Jefferies C, Cryan SA. Targeted liposomal drug delivery to monocytes and macrophages. J Drug Deliv 2011;2011:727241.

[29] Balch CM, Soong SJ, Gershenwald JE, Thompson JF, Reintgen DS, Cascinelli N, *et al.* Prognostic factors analysis of 17,600 melanoma patients: Validation of the American joint committee on cancer melanoma staging system. J Clin Oncol 2001;19:3622-34.